Analysis of the Behaviour of an Optimized Magnetorheological Brake

Giuseppe Marannano[1]; Gabriele Virzi' Mariotti[2]; Cedomir Duboka[3]

[1,2] Dipartimento di Ingegneria Chimica, Gestionale, Informatica, Meccanica Università di Palermo, Viale delle Scienze 90128 Palermo, Italy, [3] University of Belgrade, Faculty of Mechanical Engineering, SRB-11120 Belgrade 35, K. Marije 16, Serbia

[*1]giuseppe.marannano@unipa.it; [2]gabriele.virzimariotti@unipa.it; [3]cduboka@eunet.rs

Abstract

This paper presents the optimization process of MR – magnetorheological brake in order to define its configuration, and to reach the requested vehicle braking torque. FEM analysis previously carried out, concerning structural sizing of such a brake, showed that both braking torque and brake mass did not satisfy the requirements. Due to the necessity of limitation on the suspended mass of a motor vehicle, the optimization of the form of MR brake stator has been executed, including determination of its contribution to the total mass of the brake. Thus a percentage reduction of approximately 40% was obtained. In order to estimate the brake temperature which results from the transformation into heat of a vehicle kinetic energy during brake application, a thermal Finite Element Analysis is carried out. In particular a fade braking test composed of snub braking, i.e. repeated cycles of acceleration and consecutive braking applications is performed.

Keywords

Magnetorheological Brake; FEM Optimization; Magnetic FEM; Thermal FEM; Fade Braking Test

Introduction

Sizing of MR brake was executed in the preliminary work (Marannano, Virzì Mariotti and Duboka, 2011), following the criteria available in the literature (York, 1997; Carlson LeRoy, Holzheimer, Prindle, Marjoram., 1998). The requirements (Carlson, 1999; Brauer, 2006) for an automotive brake were not found to be satisfied in this way. In fact FEM Analysis, performed on the model of MR brake, reveals the possibility to bring modifications to the magnetic circuit, with the aim to improve the requested performances, in terms of the maximum braking torque value and the minimal weight of the device.

The procedure of MR brake design is studied, and several papers are found in the literature (Karakoc, Park and Suleman, 2008; Farjoud, Vahdati and Fah, 2008; Yang, Huang and Kang, 2007; Li and Du, 2003; Liu, Li, Kosasih and Zhang, 2006; Park, Stoikov, da Luz and Suleman, 2006; Sukhwani and Hirani, 2008; Zhou, Chew and Hong, 2007). Several modifications on the original procedure have been proposed, but the FEM Analysis showed that the analytical procedure did not enable the values of the required braking torque to be obtained. Additional optimization is carried out, to obtain the achievement of requirements (Yang, Duan and Eriksson, 2008; Jaindl, Köstinger, Magele and Renhar, 2007; Park. Luz and Suleman, 2008).

Compared to similar analyses found in literature, MR brake in present research consists of two discs instead of one (Nguyen and Choi, 2011); in order to contribute to the feasibility of the brake design. Magnetic circuit optimization process is executed in two phases, using parametric FEM model of the brake. The primary objective of the first phase is the determination of the optimal geometric parameters of the magnetic circuit, to obtain values of braking torque not lower than the nominal (or designed) value - Mfnom, representing the limit of a typical motor vehicle brake. Starting from the obtained configuration, the second phase of optimization was deemed to search an optimal form of the stator in ferromagnetic steel that is the novelty regard to previous works. The decreasing trend of the magnetic induction B versus the decreasing distance from the rotation axis suggests a shape of variable thickness of the stator that is modeled by a spline, while the coordinates of the control points are chosen as design variables; thickness of MR fluid (ξ = 1 mm) is not modified during the optimization procedures. Thus a sensitive reduction of the mass of the entire MR brake may be obtained, without significant reduction of the braking torque performance, to acquire very original shape of the brake geometry, with simultaneous achievement of requirements in terms of both brake torque and mass.

Finally the fade behaviour of the brake is analysed from the viewpoint of dynamic thermal analysis, to simulate a braking test with the maximum temperatures that significantly affect the efficacy of MR fluid (Nguyen and Choi, 2011, Park, Luz and Suleman, 2008; Wiehe, Noack and Maas, 2007).

Optimization process

The process of optimization (Kodiyalam and Saxena, 1994) of an element consists of search on a whole of design variables (state variables), minimum value assumed by a determined objective function, and satisfication of the requirements demanded by the system. The mathematical formulation of a typical process of optimization is:

$$\begin{aligned} &\textit{Minimizing} \quad f(\{x\}) \\ &\textit{Subjected to:} \quad g_j(\{x\}) \le 0 \qquad j = 1,2,\dots m \\ &\textit{being:} \quad \begin{cases} x_{i,\min} \le x_i \le x_{i,\max} \\ \{x\} = [x_1, x_2 \dots x_n] \end{cases} \quad i = 1,2,\dots n \end{aligned} \tag{1}$$

where $f(\{x\})$ represents the objective function, $\{x\}$ is the vector of independent variables of design, in number equal to *n*, subjected to constraints imposed by $[x_{i,\min}, x_{i,\max}]$, while $g(\{x\})$ represents the whole of state variables, in equal number to *j*, functions of the design variables that the system must satisfy.

Therefore the optimization represents a procedure pointing out the best design variables, inside an admissible domain, that render minimum (or maximum) a determined function of the variables governing the problem.

The search for "an optimal" solution to the problem can be take advantage of a great variety of methods. The choice of the method is a direct consequence of the type of problem under investigation.

A distinction is done between problems of conditioned type, in the admissible design configuration with respect of imposed conditions (constraints), and problems of unconditioned type that have not restrictions. This last have simpler solution but rare presence in engineering (Nocedal and Wright, 2006), (Elster, 1993). However, several methods may be used to transform a problem of conditioned type in unconditioned one (method of the penalty functions).

Another important factor concerns the existence of eventual local minimums of the objective function. Such type of problem can be resolved by means of various methods, among which the execution of several analyses are started by a whole of design variables inside the permissible domain. A complete description of the state variables is presented in the next paragraphs 3.1 and 3.2.

1) Ansys optimization

ANSYS executes a series of cycles of analysis-appraisal-modification of the model testing in an iterative way the design variable (DV), state variable (SV) and the objective function (OBJ). Such variables are defined in parametric way, by means of language *ADPL*. The constraints on both the design and the state variables are imposed by the user. Their choice, with that of the objective function, represents one of the most important elements of the decision phases to really obtain a solution that represents the optimal design. A whole of values of design variables satisfying the imposed constraints for the problem under investigation, is indicated like *feasible* by the software; otherwise it is indicated as *infeasible* and eliminated by the whole of the solutions. The optimization procedure uses the method named *Subproblem approximation method*, for the minimization of the objective function. The software uses some techniques of optimization, by means of which the efficiency of the process is increased and the *design random generation* is used. The better solutions constituting the point of departure for the successive procedure of optimization, may be selected by means of the instruction *OPSEL*.

First phase of optimization of the magnetic circuit

The first step of the optimization process of the magnetic circuit regards the choice of the objective function and the design variables, with the determination of the constraints (variables of state).

The primary objective is the determination of the best geometry of the magnetic circuit to obtain a value of braking torque equal to requested nominal value Mf_{nom}. An objective function must be imposed that considers *feasible* the geometrical configurations of the circuit, for which the condition $M_f \ge M_{fnom}$ is fulfilled, being M_f the actual braking torque.

The objective function is defined in the form:

$$f(x) = K - M_f \tag{2}$$

The term K in (2) represents a constant, introduced with the aim to avoid numerical problems, due to negatives values of $f(x)$ during the optimization process. A value much greater than the braking torque, equal to 10^4, is chosen.

An important aspect is the mass of the brake, which has to assume to be the lowest possible values, because too heavy brake greatly increases the overall weight of the vehicle. Since the total mass of the brake is mainly determined by the size of the magnetic circuit (greater density of ferromagnetic steel and of the copper of the coil), a maximum acceptable limit has to be considered, by introducing the state variable:

$$P \leq P_{\max} \qquad (3)$$

Value of Pmax fails to reduce the search domain of the optimal solution. Referring to the mass value of the model, obtained from a first approximate sizing, a maximum value of Pmax=0,8 P= 33,8 kg is imposed. The ratio 0,8 is not exclusive and the objective is a lower mass than the initial one. If a lower value of the ratio is chosen, the same value of the mass is obtained as the final result.

Mass of the MR brake can not be compared to the hydraulically or mechanically operated braking systems which are characterized with the presence of additional components (brakes pump, oil tank, hydraulic circuit, mechanical linkage, etc.) replaced by electrical components in the case of MR brake. Another constraint is the upper limit of the magnetic field B in the stator steel. Indeed, if the value of magnetic field in steel C10 is close to the saturation value, the circuit is unable to produce an increase in the magnetization of the MR fluid, increasing the current supplied to the system. This causes loss of linearity in the electromechanical characteristic (torque-current) of the device. A state variable is then defined taking into account the saturation of steel, assuming the following expression:

$$B \leq 0{,}9 \cdot B_{sat} \qquad (4)$$

TABLE 1 DESIGN VARIABLES AND RELATIVE CONSTRAINTS.

Design variables	*Range of variation [mm]*
Inner radius of active surface r_i	40-140
Radial thickness of the coil L_c	5-20
Disk thickness s_d	2-10
Stator radial thickness S1	5-30

The choice of the limits within which the design variables change takes into account two factors. On one hand too large range do not adequately represent the entire admissible domain, while on the other hand too narrow range may exclude the best solutions. The selected design variables and their range of variation are listed in Table 1.

TABLE 2 RESULTS OF THE FIRST PHASE OF OPTIMIZATION.

Objective function	*Obtained values*
Braking torque [Nm] Mass [kg]	1055,34 29,75
Design Variables	*Optimal values [mm]*
Inner radius of active surface r_i Coil radial thickness L_c Disk thickness s_d Stator radial thickness S_1	133,5 9,2 3,2 15,34

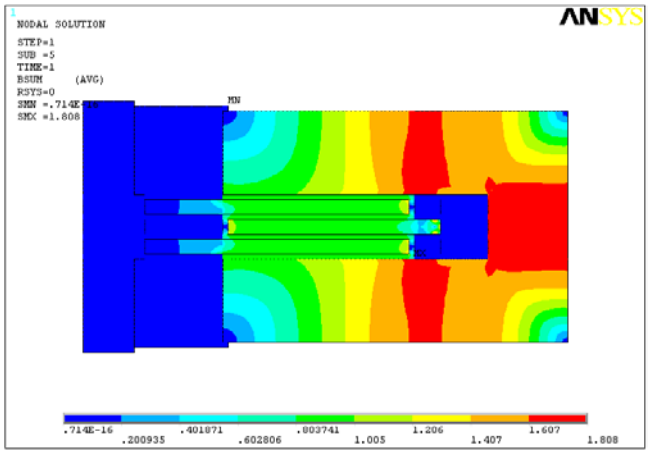

FIGURE 1 MAGNETIC FIELD DISTRIBUTION.

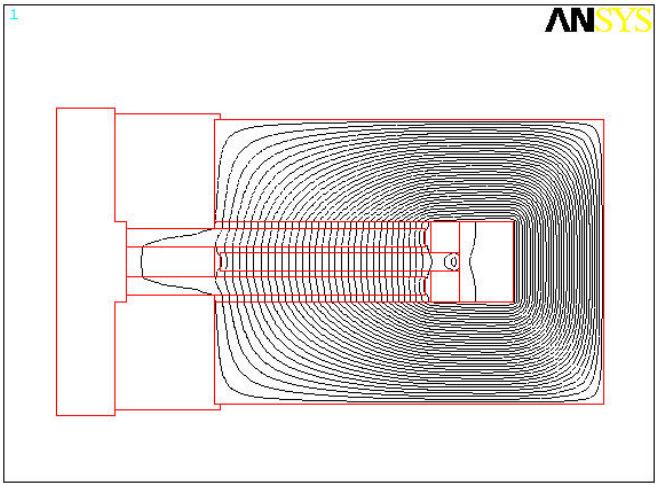

FIGURE 2 FLOW LINES.

1) *Results*

Table 2 shows the results of the first phase of optimization of the magnetic circuit, where the best configuration is reported. Analysis of Table 2 shows that, in the best configuration, the MR brake is capable to generate a value of braking torque above the minimum required. The mass of the brake is lower than the preset limit and the reduction is approximately 30% compared with the value obtained from the preliminary analysis.

Figure 1 shows the distribution of magnetic field in the circuit in the optimal solution. The maximum value of Bf at the fluid gap is now equal to $B_f \cong 0{,}8\,T$, which is sufficient to obtain the required magnetization. Fig. 2 shows the flow lines of magnetic field.

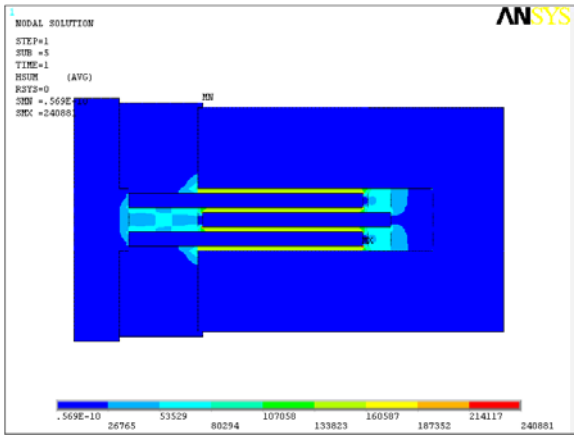

FIGURE 3 MAGNETIC FIELD INTENSITY H.

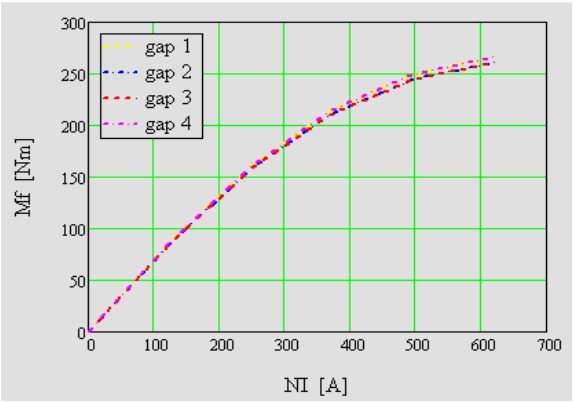

FIGURE 4 BRAKING TORQUE VERSUS *NI* FOR EACH ACTIVE SURFACE (FIRST OPTIMIZATION).

Figure 3 shows the map of the intensity of magnetic field H in the circuit. The mean value of magnetic intensity is equal to Hf ≅ 140 kA/m, corresponding to a shear stress τH ≅ 52 kPa, which is very close to the maximum shear stress of MR fluid. Figure 4 shows the load variation versus the magnetomotive force (NI) supplied to the system, obtained from interpolation of data for each active surface. An almost identical trend can be observed for each pair of external (gap 1 and 4) and internal (gaps 2 and 3) gaps. The contribution of each gap to the value of total braking torque is slightly higher for each gap on the outside, near to the maximum value of magnetomotive force. The electromechanical characteristic of the brake may be estimated adding the contributions of braking torque for each gap fluid, as Figure 5 shows.

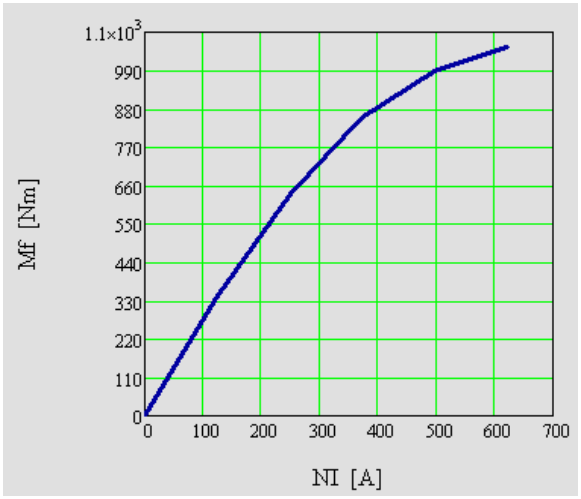

FIGURE 5 ELECTROMECHANICAL CHARACTERISTIC OF THE BRAKE (FIRST OPTIMIZATION).

The torque has a roughly linear trend to vary NI, except the last section where the curve decreases its slope. This completely predictable behaviour is due to values of current near to the maximum value, so that the magnetic field in the circuit tends to reach the saturation value of ferromagnetic steel.

Braking torque assumes the value to be zero in the absence of applied current; due to the fact that the contribution of the Newtonian term of the shear stress is neglected in the calculation of total braking torque.

Torque $M_{f\eta}$ due to viscosity in lack of magnetic field is given by:

$$M_{f\eta} = \frac{\pi}{2} \cdot \frac{\eta}{\xi} \cdot \omega \cdot (r_e^4 - r_i^4) \qquad (5)$$

Where η = 0,280 Pa is the viscosity, ξ = 0,001 m is the gap, ω is the angular velocity (which is equal to 118,2 rad/s for initial speed of 120 km/h and the tyre rolling radius of 0,282 m), r_e and r_i are external and internal radius of the disk respectively. A value of the torque equal to 33 Nm is thus obtained; that is 3,1% of the value reported in table 2.

Second phase of magnetic circuit optimization

Figure 1 shows that the stator in ferromagnetic steel is characterized with regions at low density of magnetic flux. In particular, the value of B decreases in radial direction towards the regions near to the axis of rotation of the brake. For the principle of continuity of magnetic flux, considering two generic sections of the stator, one has:

$$\phi_1 = \phi_2 = B_1 \cdot A_1 = B_2 \cdot A_2 \qquad (6)$$

Since the value of magnetic field B is inversely proportional to the size of the section crossed by the flow, the thickness of the stator can be reduced in axial direction in zones where B is low, compared to the magnetic saturation of the steel.

In light of these considerations, the second phase of the optimization process is useful to find a suitable form of the stator, to reduce the mass without affecting the system performance significantly.

1) Changes to FEM model

A modification of the geometry of the model is necessary to search an optimal form of the brake stator. The stator is achieved in a completely parameterized way by means of bottom up procedure. The outer contour is achieved by the use of Spline Curves, passing through checkpoints set. This approach allows obtaining an external profile of the stator, through the variation of the vertical coordinate of these points. The procedure has already been described in the previous paragraph, so that the intermediate steps are the same; the optimization parameters are indicated in the next paragraph.

The active surfaces of the model are implemented in parametric form by direct generation of nodes and elements for the subsequent calculation of the braking torque. Figure 6 shows the geometry of the brake, the control points and the stator thickness.

2) Definition of the optimization parameters

Since the second phase of optimization is devoted to the research of the lower mass of the brake, the objective function is represented by this variable:

$$f(x) = P \qquad (7)$$

Changing the shape of the stator as well leads to an increase in the value of the magnetic field passing through it. This leaves an increase of the total reluctance of the circuit, reducing the intensity of magnetization in MR fluid. The introduction of the new state variable is necessary.

$$M_f \geq M_{fnom} \qquad (8)$$

to avoid the reduction of the performance requirements in terms of torque produced by the brake. The number of design variables is greater compared to the previous optimization. The establishment of the stator thickness at control points requires some essential considerations, because their variation during the optimization process cannot be arbitrary, to avoid geometric configurations that may be difficult to implement.

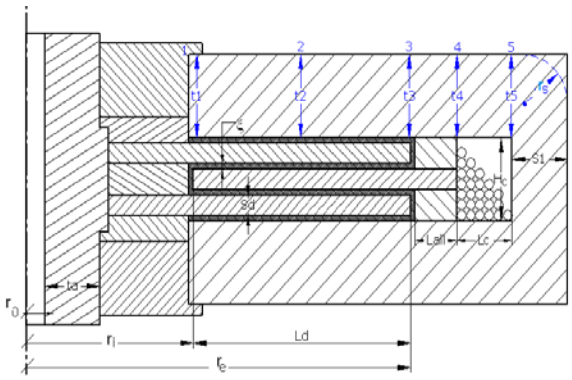

FIGURE 6 CONTROL POINTS IN THE BRAKE GEOMETRY.

TABLE 3 DESIGN VARIABLES AND CONSTRAINTS.

Design variables	*Variation range [mm]*
Inner radius of active surface r_i	40-140
Coil radial thickness L_c	4-12
Disk thickness s_d	2-8
Stator radial thickness S_1	5-20
Stator axial thickness t_1	4-10
Increase Δ_1	0-5
Increase Δ_2	0-5
Increase Δ_3	0-3
Stator axial thickness t_5	8-20
Fillet radius r_s	3-12

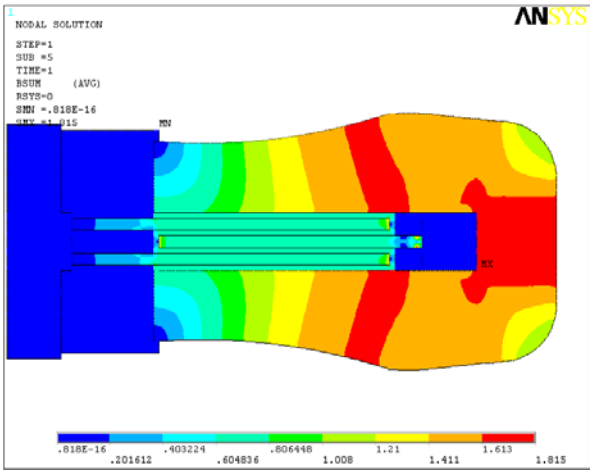

FIGURE 7 DISTRIBUTION OF THE MAGNETIC FIELD *B* IN THE SECOND OPTIMAL CONFIGURATION.

The decreasing trend of the magnetic field through the stator (Fig. 1) suggests, like possible configuration, a stator thickness gradually growing in radial direction away from the axis of rotation. On that basis, a dependency relationship between the control thicknesses from t_1 to t_4 may be established, in order to obtain really feasible results of the optimization. In particular, for given value of t_1, the following relationship is imposed:

$$t_{i+1} = t_i + \Delta_i \qquad i = 1 \ldots 3 \qquad (9)$$

Δi represents the successive increase in thickness, giving a tapered form towards the outside of the stator. Table 3 shows the selected design variables and their ranges of variation established according to the results obtained from the first phase of optimization.

Maximum radius of the brake is Rmax = 200 mm and thickness of MR fluid is ξ = 1 mm; excluding from modification during optimization procedure.

3) Results

Table 4 shows the results obtained for the geometry optimization. The second phase of optimization allows a reduction of brake mass of about 14% compared to the value obtained in the first phase. It is also important to note that, despite the increase of the reluctance of magnetic circuit, due to the increase of the magnetic field B, the value of braking torque is reduced by less than 3,5%. Figure 7 shows the distribution of the magnetic field in the circuit, in the plane. The maximum value of B in the stator is greater than the previous, but lower than the limit of saturation of the steel.

TABLE 4 RESULTS OF THE SECOND PHASE OF OPTIMIZATION.

Braking torque [Nm] Mass [kg]	1020 25,8
Design variables	*Optimum values [mm]*
Inner radius of active surface r_i Coil radial thickness L_b Disk thickness s_d Stator radial thickness S_1	126,8 10 2,5 14,6
Stator axial thickness t_1 Stator axial thickness t_2 Stator axial thickness t_3 Stator axial thickness t_4 Stator axial thickness t_5 Fillet radius r_s	12,2 12,8 17,1 17,1 16,2 10

Figures 8 and 9 show the electromechanical characteristic of the new configuration, both for individual disks and the entire brake, in a similar way to the previous optimization phase.

Thermal analysis of the MR Brake

Working principle of the MR brake foresees the presence of sliding between the active surfaces in relative motion. It must be able to get over a determined value of mechanical power in heat, arousing the increase of the temperature of MR fluid. Determination of the temperature distribution is very important, given that MR fluid works under a limited temperature range.

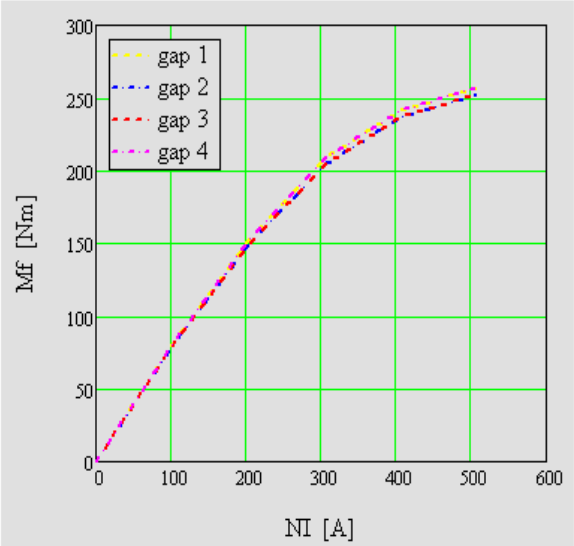

FIGURE 8 BRAKING TORQUE VS *NI* FOR EACH ACTIVE SURFACE (SECOND OPTIMIZATION).

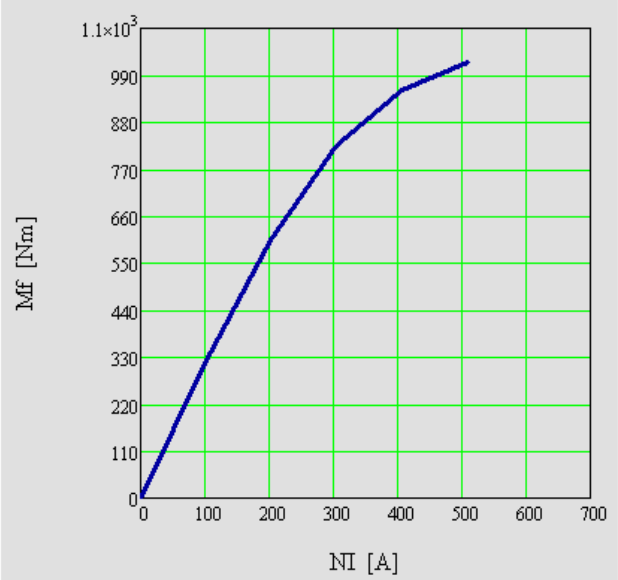

FIGURE 9 ELECTROMECHANICAL CHARACTERISTIC

Considerations on the thermal equilibrium of the system are useful for a better clearness.

The heat exits from the system through a convection exchange, while the energy enters under mechanical form, for effect of the sliding between the rotary parts, or under electrical form, for Joule effect due to the current in the coil. Under these conditions, the heat balance is:

$$\dot{Q} - \dot{W} = \frac{dU}{dt} \qquad (10)$$

where $\dot{Q}$ is the heat quantity transferred outside in the time unit, $\dot{W}$ is the energy in the unit time and dU/dt is the variation of the inner energy of the system. One has:

$$\dot{Q} = -h \cdot A_s \cdot [\theta(t) - \theta_0] \quad (11)$$

h is the convection coefficient, $\theta(t)$ and θ_0 represent respectively the temperature in function of the time and the temperature of environment, while A_s is the outer surface affected by the convection flow. The power entering in the system can be expressed as:

$$\dot{W} = -P_{MR} - P_{el} \quad (12)$$

P_{MR} is the mechanical power dissipated by the brake and P_{el} represents the electrical power supplied by the winding. The variation of inner energy of the system can be written as:

$$\frac{dU}{dt} = \frac{d\theta}{dt} \cdot \sum m_i \cdot c_{p,i} \quad (13)$$

$d\theta/dt$ is the temperature gradient, while $\sum m_i \cdot c_{p,i}$ represents the sum of the thermal masses of the system that is the product between the mass of every component and own specific heat. The heat balance of the brake is:

$$-h \cdot A_s \cdot [\theta(t) - \theta_0] + (P_{MR} + P_{elettr}) = = \frac{d\theta}{dt} \cdot \sum m_i \cdot c_{p,i} \quad (14)$$

That is a differential equation of the first order at variable coefficients.

1)Determination of the heat flux in the braking

The heat generated during braking is due to the dissipation of both the mechanical power and the electrical power supplied by the winding for Joule effect.

The appraisal of the heat flux generated during the relative motion between the surfaces of the rotor and of the stator in contact with MR fluid, can be determined calculating the variation of kinetic energy of the vehicle under braking. Based on the characteristics of the vehicle, assuming initial speed equal to V = 120 km/h (33,3 m/s), kinetic energy variation in braking until the stop is:

$$\Delta E_k = k_a \frac{1}{2} m_v \cdot V^2 \quad (15)$$

k_a the inertia coefficient that takes in account also the inertia of the rotary mass is a function of the transmission ratio. Moreover the percentage of braking for every front brake may be calculated taking into account the distribution of braking force on the axes. The power in braking can be calculated depending on the time of braking. At last, the power transformed on heat for Joule effect in the coil has to be added:

$$P_{el} = \rho_{Cu} \cdot J_{\max}^2 \cdot V_b \quad (16)$$

V_b is the volume of the coil obtained by the optimization, while $\rho_{Cu} = 1{,}7 \cdot 10^{-8} \Omega m$ is the electric resistivity of the copper at 20°C and J_{max} is the current density. Contribution of this term is negligible in comparison with the previous.

TABLE 5 PHYSICAL PROPERTIES OF MR140CG LORD CORPORATION.

Base Fluid	Oil hydrocarbon
Color	Dark gray
Working temperature (°C)	-40 - 130
Viscosity (Pa·s)	0,280
Density (kg/m³)	3540
Weight percentage of particles	85,44%

2) FE thermal analysis

Thermal analysis of the brake is implemented using the geometry obtained from the optimization process. The software demands the insertion of the thermal properties of the materials. The properties of the MR fluid are reported in Table 5, while Table 6 reports the properties of other materials.

The loads and the boundary conditions are the power dissipated during the braking and the convective exchanges between the external surface of the brake and the environment. The dissipated power is introduced into *Ansys* like specific power in correspondence with the active surfaces of MR fluid. The simplificative hypothesis can be made that the heat generated for unity of surface is uniformly distributed, although the value of tangential stress in the fluid and the correspondent development of heat is variable (Cengel, 2007; Wiehe, Noack and Maas, 2009). In effects, the thermal flow is proportional to tangential stress that is a function of the intensity of magnetic field, and is proportional to the relative speed between the surfaces, so that the variables are numerous. A more accurate calculation that takes in account the variation of all the quantities, can be a successive development for a more precise temperature

calculation

TABLE 6 MAIN PROPERTIES OF THE BRAKE MATERIALS.

Properties	*C10*	*AISI 304*	*Al T6061-T6*	*Copper (of the coil)*
Composition	C 0,08-0,13% Fe 99,1-99,6% Mn 0,3-0,6%	C 0,08% Cr 18-20% Fe 66-74% Mn 2% Ni 8-10,5%	Al 95,8-98,6% Cr 0,04-0,35% Cu 0,15-0,4% Fe 0,7% Mg 0,8-0,2%	
Density (kg/m³)	7860	8000	2700	8920
Yield strength (MPa)	305	215	276	48
Ultimate strenght (MPa)	365	505	310	216
Elastic modulus (GPa)	205	193	68,9	117
Poisson ratio	0.29	0.29	0,33	0,355
Thermal Conductivity (W/m·K)	49,8	16,2	167	140
Specific heat (J/Kg·°C)	448	500	896	385

Usually it is difficult to determine the convection coefficient, being depending on the dimensions of the surface of heat exchange, the speed of the air and its density, dynamic viscosity, thermal conductivity and specific heat. The existing relations for the determination of the value of *h* are various, based on the calculation of characteristic numbers in dimensionless form. The condition can be assumed for the brake under investigation that the heat exchange is of forced type and the speed of the air at the external surface is equal to that of translation of the vehicle. Convection coefficient can be determined by the following relationship:

$$h = \left(\frac{\lambda}{D}\right) \cdot Nu \qquad (17)$$

where λ is the thermal conductivity of the air equal to λ = 0,0253 W/m°C at 20°C and *Nu* is the number of Nusselt, that is function of both Reynolds variable and Prandtl number Pr=0,714 *(20°C).* Density and viscosity of the air are respectively, at 20°C:

$$\rho_a = 1{,}224 \frac{kg}{m^3} \quad \eta_a = 1{,}8 \cdot 10^{-5} \frac{kg}{m \cdot s} \qquad (18)$$

Relationship (18) referred to the case of a cylinder having circular section, is useful for this type of brake; in addition Figure 10 shows the trend of convention coefficient versus the vehicle speed.

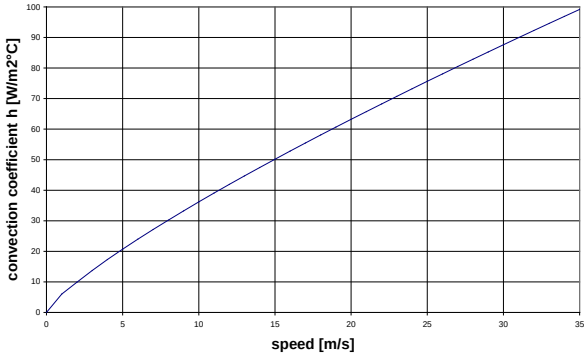

FIGURE 10 CONVECTION COEFFICIENT VS VEHICLE SPEED.

3) Dynamic analysis

Typical test, in order to estimate the efficiency of the brakes of traditional type, is taken in consideration to simulate the real working of the brake (Aleksendric, Duboka, Gotowicki, Nigrelli, and Virzì Mariotti, 2006). Fifteen brake applications with a speed of 120 km/h till the full stop of the vehicle, are executed with the constant deceleration |a| =0,75 g and a braking time t_f =4.53 *s* and every single stop is followed by an acceleration period of the duration 28 s till a speed 120 km/h. The employed time in order to complete each of the 15 cycles is equal to t_{cycle}=32.53 s. Table 7 shows the detailed list of the test for every cycle. The total time of the test is t_{test}=488 s = 8.13 min, while the covered distance is s_{test} = 8129,7 m.

TABLE 7 DETAILED LISTS OF THE BRAKING TEST FOR SINGLE CYCLE.

Time [s]	*Speed [km/h]*	*Space [m]*
0	0	0
28	120	466,48
28+4,53=32,53	0	541,98

Ansys dynamic analysis demands the load definition and the boundary conditions in function of the time. It is necessary to subdivide the cargo history in successive *loadsteps* that the software resolves in sequential way to determine the temperature distribution in the brake during the entire test.

During the phase of acceleration, in the hypothesis to neglect the friction and the generated heat due to the viscosity of the fluid, the brake is considered

subjected to convection exchanges with the environment.

System is subjected to the heat load during the braking phase, due to the power dissipated in correspondence of the active surfaces and to the convection exchanges with the surrounding, having temperature θ_0=20°C. Figure 11 shows the course of the maximum temperature in the brake versus the time for the entire test.

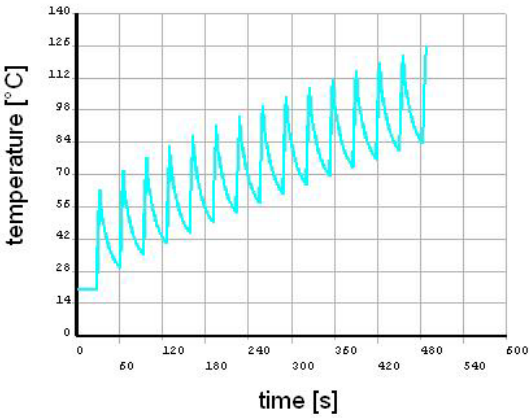

FIGURE 11 MAXIMUM TEMPERATURE IN THE BRAKE DURING BRAKING TEST.

Temperature ascends quickly during the braking phase for every braking cycle, while declining in correspondence of the phase of acceleration, the brake disperses heat for convection. The final temperature to the end of the 15 cycles is equal θ_{fin}=125,5°C, which is lower than the value of the temperature limit of working of the MR fluid θ_{max}=150°C. Figure 12 shows the map of the distribution of the temperature in the brake to the end of the test. The maximum temperature in the brake at the end of the test is in correspondence to the inner layers of MR fluid. This is mainly due to the difficulty of loss of heat in such zones. Too much high temperatures could be obtained in the fluid, such as to compromise the correct operation, in more severe conditions of exercise (greater number of cycles and more elevated speeds). A cooling system that makes easy the removal of produced heat has fundamental importance.

Conclusions

The optimization procedure of MR brake has been carried out in order to verify its ability to satisfy both braking torque and mass requirements for a vehicle brake. The obtained results of thermal analysis highlight a maximum temperature within the limit operating value of the fluid. However, cooling of the brake to remove the heat over the active surfaces is necessary in the hypothesis of employment of the brake in more severe conditions of application. This could be put into effect to achieve fins in the stator, that increase the surface of thermal exchange with the environment, or a cooling of "active" type, taking advantage of the system already presented on the vehicles.

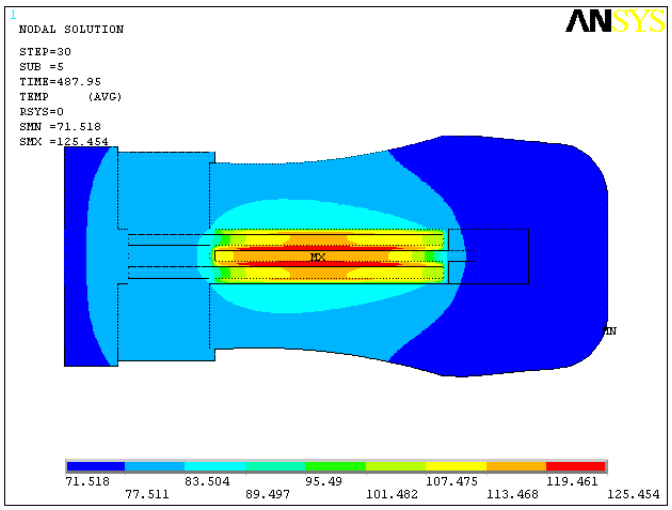

FIGURE 12 TEMPERATURE DISTRIBUTION AT THE END OF THE BRAKING TEST.

Advantages derived from the use of MR brake in place of a conventional brake (disc or drum) for motor vehicle are significant. In the first instance, MR brake provides reduced response time compared to hydraulically and/or air operated brake and it takes some time to raise the line pressure of the fluid to initiate braking. The greater response time brings reduction of the space, making, therefore, braking results more effective. The substitution of the conventional hydraulic braking system with an electrically operated system offers advantages in terms of simplicity of configuration and better solutions of housing.

Possible future developments of MR brake deal with the choice of the bearings to be used between rotor and stator, and a complete design of the devices of seal of the fluid, in order to avoid potential losses, without compromising braking efficiency. It is moreover important to emphasize that the seals have not to be attacked by the magnetic flux, in order to avoid the solidification of MR fluid in their proximity with consequent damaging.

Future developments of this work are:

- the study of the reduction of motion resistance due to the viscosity of MR fluid under normal operation, implementation

of a gap of variable thickness introducing spider legs or other. The results can be improved by making use of CFD.

- set up an analytical model or tool to predict thermo-dynamic behaviours of MR brake and build a working prototype to verify the performances.

REFERENCES

Aleksendrić D., Duboka Č., Gotowicki P. F., Nigrelli V., Virzì Mariotti G. 2006, "Braking Procedure Analysis of a Pegs-Wing Ventilated Disk Brake Rotor", Int. J. Vehicle Systems Modelling and Testing, Vol. 1, No 4, pp 233-252.

Brauer, J.R., 2006, "Magnetic Actuators and Sensors", John Wiley & Sons,.

Carlson, J.D., LeRoy D.F., Holzheimer J.C., Prindle D.R., Marjoram R.H., 1998, "Controllable brake", US Patent 5,842,547, Lord Corporation.

Carlson, J.D., November 1999, "Magnetic Circuit Design", Engineering note, Lord Corporation, Materials Division.

Cengel Y. A., 2007, "Introduction to Thermodynamics and Heat Transfer + EES Software", McGraw Hill Higher Education, London, ISBN: 0077235657

Elster, K.H., 1993, "Modern Mathematical Methods of Optimization", Wiley Vch, London, ISBN 3-05-501452-9.

Farjoud, A., Vahdati, N., Fah, Y.F., 2008, "MR-fluid yield surface determination in disc-type MR rotary brakes", Smart Materials and Structures, vol. 17, no. 3, art. no. 035021.

Jaindl, M., Köstinger, A., Magele, C., Renhart, W. 2007, "Optimal design of a disk type magneto-rheologic fluid clutch", Elektrotechnik und Informationstechnik, vol. 124, no. 7-8, pp. 266-272.

Karakoc, K., Park, E.J., Suleman, A. 2008, "Design considerations for an automotive magnetorheological brake", Mechatronics, vol. 18, no. 8, pp. 434-447.

Kodiyalam, S., Saxena, M (edit.), 1994, "Geometry and Optimization Techniques for Structural Design" Elsevier Applied Science, London, ISBN 1-85312-234-3

Li, W.H., Du, H. 2003, "Design and experimental evaluation of a magnetorheological brake", International Journal of Advanced Manufacturing Technology, vol. 21, no. 7, pp. 508-515.

Liu, B., Li, W.H., Kosasih, P.B., Zhang, X.Z. 2006, "Development of an MR-brake-based haptic device", Smart Materials and Structures, vol. 15, no. 6, pp. 1960-1966.

Marannano, G.V.; Virzì, Mariotti G., Duboka, C. 2011; "Preliminary Design of a Magnetorheological Brake for Automotive Use", Proceedings of the 23th JUMV International Automotive Conference, JUMV-SP-1101, Belgrade, 19-21 April 2011.

Nguyen, Q.H., Choi, S.B. 2010 "Optimal design of an automotive magnetorheological brake considering geometric dimensions and zero-field friction heat" - Smart Mater. Struct. 19 115024 (11pp) doi:10.1088/0964-1726/19/11/115024

Nocedal, J., Wright, S.J., 2006, "Numerical Optimization" Springer, London, ISBN 0-387-30303-0.

Park, E.J., da Luz, L.F., Suleman, A. 2008, "Multidisciplinary design optimization of an automotive magnetorheological brake design", Computers and Structures 86 (3-5), pp. 207-216

Park, E.J., Stoikov, D., da Luz, L.F., Suleman, A. 2006, "A performance evaluation of an automotive magnetorheological brake design with a sliding mode controller". Mechatronics, 16, pp. 405–416.

Sukhwani, V.K., Hirani, H. 2008, "Design, development, and performance evaluation of high-speed magnetorheological brakes", Proc. IMechE, Part L: Journal of Materials: Design and Applications, vol. 222, no. 1, pp. 73-82.

Wiehe, A., Noack, V., Maas, J., 2009, "A Model of Heat Dissipation for MR based Brake", 11th Conference on Electrorheological Fluids and Magnetorheological Suspensions IOP Publishing, Journal of Physics: Conference Series **149** (2009) 012084 doi:10.1088/1742-6596/149/1/012084

Yang, L., Duan, F., Eriksson, A. 2008, "Analysis of the optimal design strategy of a magnetorheological smart structure", Smart Materials and Structures, vol. 17, no. 1.

Yang, Y., Huang, S.G., Kang, B.S. 2007, "Research on circular plate MR fluids brake", Journal of Central South University of Technology (English Edition), vol. 14, no. 1 SUPPL., pp. 257-259.

York, T.M., 1997, "Magnetorheological fluid coupling device and torque load simulator system" US Patent 5,598,908, GSE, Inc.

Zhou, W., Chew, C.-M., Hong, G.-S., 2007, "Development of a compact double-disk magneto-rheological fluid brake" Robotica, 25**,** pp 493-500 doi: 10.1017/S0263574707003372